For this device the following data were recorded:

$V_{av.} = 4.2$ volts
$I_{av.} = 2.1$ amps
$\Delta t = 2.0$ μs.

Therefore,

$$\mu_s = 17.6\ \mu\text{J}.$$

In accordance with the above criteria, the switching energy (u_s) associated with this device appears to be in the vicinity of 17.6 μJ.

References

[1] U. Milano, J. Saunders, and L. Davis, "A Y-junction strip-line circulator," *IRE Trans. on Microwave Theory and Techniques*, vol. MTT-8, pp. 346–351, May 1960.
[2] H. N. Chait and T. R. Curry, "Y-circulator," *J. Appl. Phys.*, vol. 30, p. 152 S, 1959.
[3] B. A. Auld, "The synthesis of symmetrical waveguide circulators," *IRE Trans. on Microwave Theory and Techniques*, vol. MTT-7, pp. 238–246, April 1959.
[4] H. Bosma, "On stripline Y-circulation at UHF," *IEEE Trans. on Microwave Theory and Techniques*, vol. MTT-12, pp. 61–72, January 1964.
[5] C. E. Fay and R. L. Comstock, "Operation of the ferrite junction circulator," *IEEE Trans. on Microwave Theory and Techniques*, vol. MTT-13, pp. 15–27, January 1965.
[6] L. Levy and M. Silber, "A fast switching S-band circulator utilizing ferrite toroids," *1960 IRE WESCON Conv. Rec.*, pt. 1, pp. 11–20.
[7] P. C. Goodman, "A latching ferrite junction circulator for phased array switching applications," presented at the 1965 IEEE G-MTT Symp., Clearwater, Fla.
[8] "Advanced ferrimagnetic materials applied to digital phase shifters," Air Research and Development Command, Rome Air Development Center, Griffiss AFB, N.Y., Contract AF 30(602)-3490.
[9] "Broadband junction circulators," U. S. Army Electronic Conv., prepared by Sperry Microwave Electronics Company, Clearwater, Fla, Final Rept. DA-36-039-SC-89214, May 1965.
[10] J. W. Simon, "Broadband strip-transmission line Y-junction circulators," *IEEE Trans. on Microwave Theory and Techniques*, vol. MTT-13, pp. 335–345, May 1965.

Circularly-Polarized Phase Shifter for Use in Phased Array Antennas

M. C. MOHR, MEMBER, IEEE, AND S. MONAGHAN, MEMBER, IEEE

Abstract—**An X-band, circularly-polarized, nonreciprocal, ferrite phase shifter has been developed whose size and electrical performance are favorably suited for use in transmission or reflection-type phased arrays requiring element center-to-center spacings of about 0.5 λ. The phase shifter has the same configuration as a Faraday rotator with a ferrite rod located at the center of a circular waveguide with an axially applied field. If a circularly polarized wave is passed through this geometry, a nonreciprocal phase-current characteristic is obtained. The array antenna is configured so that no phase-control field reversals are needed between transmit and receive modes of radar operation. The radiating element has been designed as an integral part of the beam steering element using waveguide array simulator techniques.**

This paper will discuss various design problems and performance of the beam steering element. A 1300-element phased array was constructed and tested. Its performance, as it relates to the phase-setting accuracy of 1300 phase-shifter constituents, is stated briefly.

I. Introduction

A MAJOR FACTOR which makes microwave phased-array antenna systems practical today is the advent of phase shifters that are suited for use as beam-steering elements. This array element requires a phaser whose cross-section size is small and its phase easily controllable. The insertion phase and controlled phase characteristic of the device must be reproducible, and because of the large quantities involved, its manufacturing-per-element-cost must be low. In addition, it must have the performance to satisfy the demands of the agile beam-antenna system application.

At microwave frequencies two general types of phase shifters are available for use as beam steering elements —diode phasers and ferrite phasers. The choice depends on the array application in mind; however, the dominating influences in the selection are the per-element specifications of operating frequency, RF power handling and switching speed. Clearly, the best choice of a phase shifter for use in a phased-array application cannot be made without a system tradeoff considering all components between the beam-steering computer input and phase-shifter output.

II. Description of Phase Shifter

The circularly-polarized (CP) ferrite phase shifter discussed in the following is a favorable technical approach for use as a beam-steering element in many array applications. Figure 1 is a cutaway view of the element cartridge showing its various functional components. Figure 2 is a photograph of the same cartridge. An array

Manuscript received May 31, 1966; revised September 8, 1966.
The authors are with the Raytheon Company, Missile Systems Division, Bedford Laboratories, Bedford, Mass.

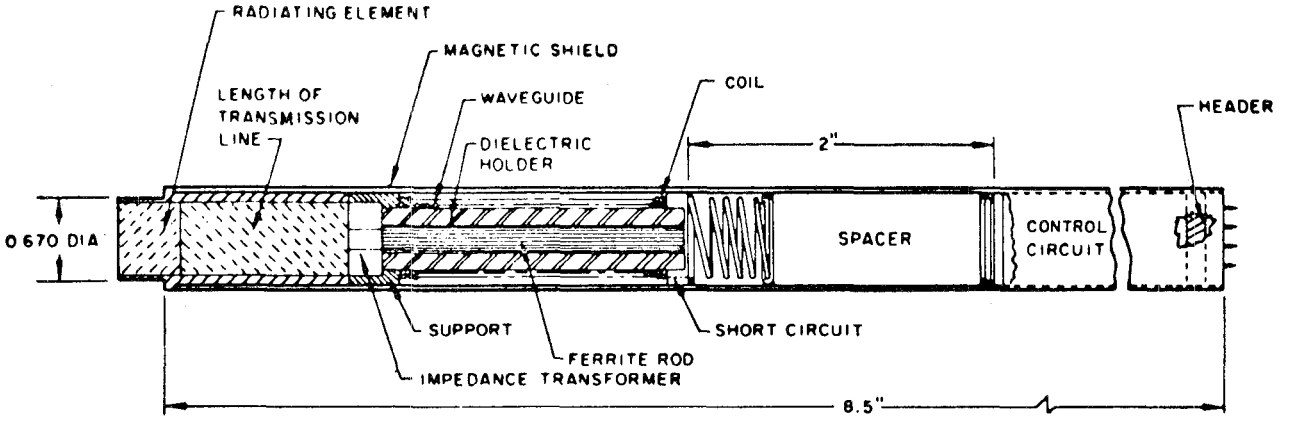

Fig. 1. Cutaway view of beam steering element.

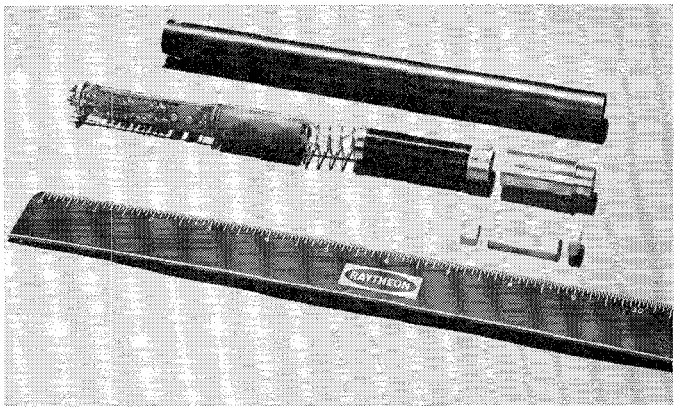

Fig. 2. Beam steering element.

antenna, which will be briefly described later, was constructed using 1300 of these devices. As can be seen in Fig. 1, the radiating element, phaser and driver circuitry is integrated into one package. This package, defined as a beam steering element, can be easily inserted or removed individually from the front face of the array, much in the same way as an electron tube is inserted or extracted from a tube socket. The header at the rear makes all the electrical control interconnections for the cartridge contained circuit and phase shifter. The ferrite rod, which is the heart of the phase shifter, is held axially by a quartz cylinder. A thin-wall circular metal waveguide is deposited on the surface of the quartz holder. The control solenoid is wound directly on the varnish protected metallized waveguide. A microwave short circuit is located at one end of the assembly making the phase shifter re-entrant. A magnetic tube serves as the cartridge container for the various parts of the beam steering element and at the same time isolates control fields between neighboring elements. The length of a circular, Rexolite-loaded transmission line can be adjusted to individually trim, and thereby guarantee reproducibility of phase shifter insertion phase. The spring is included to keep the cartridge physical length constant in spite of length changes of the trimming section. This arrangement also allows the cartridge to be assembled and disassembled with ease. Since the phased-array antenna was experimental in nature, a spacer was included in the event that in possible future configurations the cartridge-contained circuitry could be modified or enlarged. Obviously, both spring and spacer are otherwise unnecessary. The radiating element is essentially an impedance transformer that transforms the dielectric-loaded transmission line to the impedance of free space which varies with beam scan and polarization due to the ever present mutual coupling between elements in an array.

The CP phase shifter is discussed here as a reflection or re-entrant device, although it can be configured just as easily as a transmission device. The transmission and reflection CP phase shifters have been previously discussed in the literature [1], [2] so that their theory of operation is rather well known. Referring again to Fig. 1, the theory of operation can be briefly and conceptually described as follows.

The phase-shifter geometry is that of a Faraday rotator with a ferrite rod located at the center of a circular waveguide with an axially applied magnetic field. A circularly polarized signal entering the radiating element propagates through a length of transmission line and is transformed into the ferrite section where it undergoes a phase shift of $\phi/2$. The phase angle ϕ is a function of

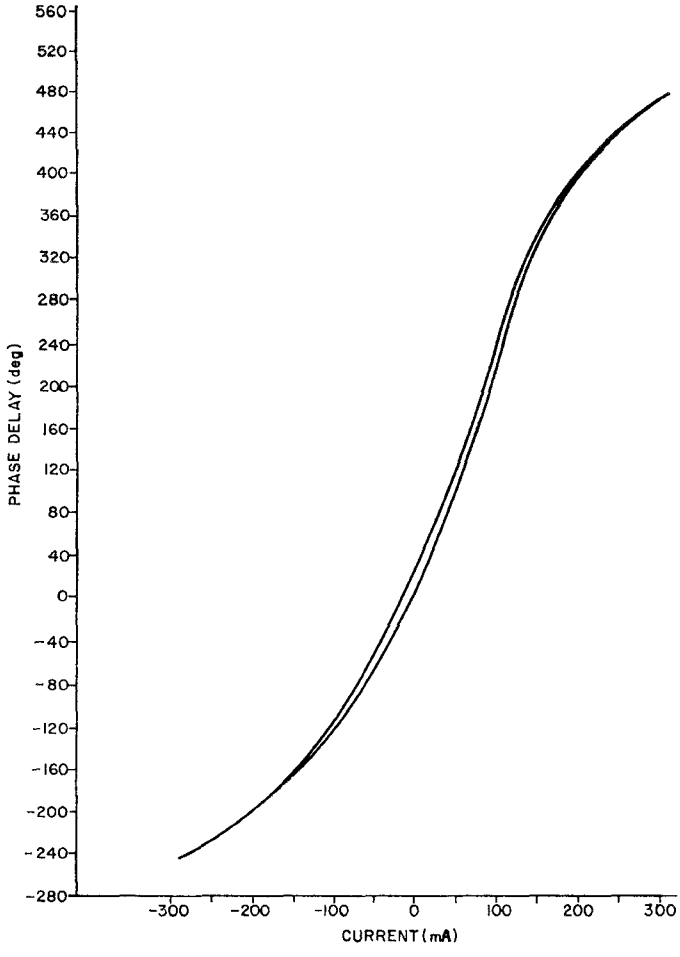

Fig. 3. Phase vs. current for one sense of circular polarization input using Raytheon R×1 ferrite material.

the applied axial magnetic control field produced by the current in the coil. The traveling wave is reflected from the short circuit and on its return path undergoes another $\phi/2$ phase shift. The wave passes through the impedance transformer and length of transmission line, and emerges from the radiating element with a total phase shift of ϕ. The phase shift in both directions is equal, since the rotation of the circularly-polarized field vector is the same for both propagation directions. The phase shift vs. coil current characteristic for the CP phase shifter used in the 1300-element array is shown in Fig. 3. Positive and negative coil currents correspond to the $u-k$ and $u+k$ scalar permeabilities, respectively. The terms u and k are the diagonal and off-diagonal terms, respectively, of the tensor permeability when one assumes a lossless ferrite medium. Since k is a negative number over the region of interest in this case, positively increasing coil currents correspond to increasing microwave scalar permeability or phase delay.

Reversing the sense of input circular polarization has the same effect on the phase-current characteristic as reversing coil current. This means that when the phase shifter is used as a beam-steering element in an array, it has the correct phase shift for only one sense of circular polarization if the variable magnetic fields are always maintained in the same direction.

If linear polarization is put into the CP phase shifter, the device behaves as a Faraday rotator according to the relation:

$$\theta = \tfrac{1}{2}[\phi(i) - \phi(-i)]$$

where θ is Faraday rotation and $\phi(i)$ is phase as a function of coil current (see Fig. 3).

III. Phase Shifter Performance

Table I is a summary list of experimentally measured CP phase-shifter performance. The sections to follow will discuss and elaborate upon each of these performance parameters.

TABLE I
PHASE SHIFTER SPECIFICATIONS

Phase range	360 degrees
Frequency	X-band ±5 percent
Insertion loss	<0.7 decibel
Maximum peak power	2.0 kilowatts
Maximum average power	35 watts
Switching speed	<10 microseconds
Switching energy (maximum current range)	50 microjoules
Maximum dc hold power	0.040 watt
Maximum hysteresis phase error (typical)	±7.5 degrees
Temperature sensitivity at zero field (insertion phase)	<0.75 degrees C
Accuracy (rms phase error, 1400 units)	<7 degrees
Weight (can be made considerably lighter)	4.9 ounces

Phase-Current Hysteresis Effects

The cutaway view in Fig. 1 describes the magnetic control circuit used to induce a field within the ferrite rod. A high permeability magnetic tube or shield covers the solenoid wound over the circular metal deposited waveguide. This tube not only serves as a container for the phase shifter, radiating element, and drive circuitry, but also provides magnetic isolation between neighboring control fields. If the control current in one phase shifter element is varied from 0 to 360 degrees, its neighboring element in the array experiences a corresponding phase variation of less than 0.2 degree.

The approximate equivalent magnetic circuit of a ferrite rod, surrounded by a coil and magnetic shield, is that of a toroid with an air gap. The air gap path in the toroid is essentially represented by leakage fields and the path between the ends of the ferrite rod and shield. The magnetic path of the toroid is crudely represented by the ferrite in series with the shield. This means that most of the magnetic energy storage occurs in the air gaps at the ends of the ferrite.

In order to simplify the phase-shifter drive circuitry it is desirable to pass current through the coil in only one direction. In addition, since linear-drive amplifiers are more desirable than those that need shaping, the ferrite rod length is adjusted to obtain a phase-current characteristic that is as close to linear as possible over a 360-degree range. For these reasons only the portion of the

curve in Fig. 3, from 10 to 177 mA, is utilized. At 177 mA coil current, the ferrite rod is operating considerably below its magnetic saturation level.

The phase shift in the CP phase shifter is related to the net magnetization of the ferrite rod. This causes the phase-current characteristic shown in Fig. 3 to exhibit a hysteresis loop. The maximum-phase hysteresis loop width is proportional to the coercive force (h_c) of the ferrite material. This assumes that the coercive force of the magnetic shield is much lower than for the ferrite. The B-H curves of an ideal toroid with no air gap, and with an air gap, are illustrated in Fig. 4. When an air gap is introduced into the closed magnetic circuit the square-loop response of B vs. H shears or pivots about the value of coercive force. The separation of the curve intersections on the B axis is a measure of the hysteresis loop width in degrees phase, since phase is related to B. This shearing of the square-loop response occurs since the air gap induces demagnetizing poles which must be overcome in order to align magnetic domains within the rod. The larger the demagnetizing field, the smaller is the hysteresis loop width. In fact, when the magnetic shield is removed, the phase hysteresis loop reduces by a factor of 2 and the coil current needed to reach the same phase increases by nearly 2. The existence of the shield around the coil effectively reduces the rod's demagnetizing field approximately by a factor of 2.

Raytheon's Research Division has developed an X-band ferrite material (RX1) which has a low coercive force of about 0.23 oersted giving a phase shifter hysteresis loop width of 15 degrees. Commercially available materials such as Trans-Tech G113 and Trans-Tech-390 have approximate coercive forces of 0.7 and 2.5 oersteds. When these two materials were measured in the same CP phase shifter design, phase-current hysteresis loops of 36 and 80 degrees were obtained as compared with 15.5 degrees with RX1.

It can be shown that errors due to a 15-degree hysteresis loop contribute less than 1.6 degrees rms phase error to the total error budget of the 1300-element array. This rms error is insignificant in an operating array of this many elements.

More recent X-band phaser designs, using shorter and fatter ferrite rods, exhibit hysteresis loop widths of 7 degrees instead of 15 degrees, but at the expense of higher switching energy.

Dc Hold Power

Maximum phase shifter hold power is defined as the coil dissipation necessary to hold the phase shifter at 360 degrees of phase or at maximum coil current. At zero phase, nearly zero current or hold power is needed. For a given phase shifter design the maximum hold power is directly proportional to the copper volume available to the control coil. This implies an obvious tradeoff between antenna maximum scan angle ability and total array hold power. This tradeoff is not too important at X-band for arrays that required a hemispherical scan sector free of grating lobes since maximum hold power is less than 40 milliwatts for this condition. At frequencies higher and lower than X-band, the tradeoff becomes more important since hold powers increase under the same conditions. The 40 milliwatt coil dissipation is considerably smaller than the dissipation in the per-element drive circuitry. Average dc driver circuit dissipation is typically 0.5 watt.

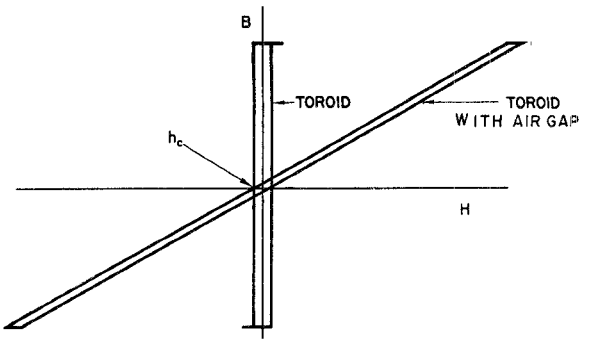

Fig. 4. B vs. H for an ideal ferrite toroid with and without air gap.

Switching Speed

In order to discuss switching speed of the CP phase shifter, it is important to define some terms. When switching the phase from one state to another, switching time will be defined as the time it takes for the RF phase to go from one phase state to within 95 percent (or 3 time constants) of its final value. For a 360-degree phase range this would correspond to the phase reaching to within 18 degrees of its final value. At this 95 percent point, the new antenna beam is well formed since the 18 degree error is maximum value of a random error function. Phase errors during the 95 to 100 percent points are random since the 1300-element array in which the phaser operates, collimates the antenna beam by inserting phase commands on the phase shifters. This has the effect of making it equally likely that any phaser in the array operates anywhere between 0 and 360 degrees for any beam position. Beam collimating is needed since the array is space fed from a point source.

The switching time of the CP phase shifter depends primarily on two factors: 1) the coil current rise or fall times, and 2) the secondary currents induced in the waveguide walls. Since the control winding for the phaser is wound directly over the waveguide wall, the wall becomes a tightly-coupled, one-turn shorted secondary. The voltage, and hence the current induced into this shorted secondary, depends on the frequency or rate of change in the drive coil current. If a step-current waveform is applied to the driver coil, the higher frequency components will induce higher currents in the waveguide wall. By Lenz's law, these induced eddy currents produce an axial magnetic field in the opposite direction to that produced by the driver coil. The result of the eddy currents is to reduce the rise time of the magnetic field within the axially mounted ferrite rod.

The simplified circuit model shown in Fig. 5 can be used to analytically relate shorted turn effects to phase-switching speed. Any distributed capacity has been assumed to be negligible. The inductance L_c is the magnetizing inductance, and the current through it is a measure of the field within the ferrite or of RF phase. The resistance R_1 is the series coil resistance. The resistance R_s is the resistance of the shorted single turn which is reflected into the transformer primary. In the transformer primary circuit the shorted turn resistance is equal to n^2R_s, where n is the number of coil turns.

The phase rise time can be found by first calculating the transfer function:

$$\left|\frac{i_c}{i_T}\right| = \frac{1}{\sqrt{1+\omega^2\left(\frac{L_c}{R_1+n^2R_s}\right)^2}}. \tag{1}$$

This is also an easy quantity to measure experimentally since i_T is the measured primary coil current and i_c represents the magnetic field within the rod in terms of frequency ω.

The switching time constant τ is easily determined by taking the inverse Fourier transform of the frequency function $i_c(\omega)$.

$$\tau = \frac{1}{\omega_c} = \frac{L_c}{n^2R_s + R_1}. \tag{2}$$

The term τ is one switching time constant. Usually R_1 is small enough to be ignored. Notice then, that shorted turn influences are independent of the number of coil turns since L_c is proportional to n^2.

In the case of the CP phase shifter under discussion here, the shorted turn resistance R_s of the circular waveguide is easily determined as:

$$R_s = R_m\left(\frac{\pi d}{l}\right) \tag{3}$$

where:

R_m = sheet resistance of the thin metal waveguide in ohms per square
d = diameter of the circular waveguide
l = length of the waveguide or ferrite rod.

The shorted turn resistance R_s is solely determined by the circular waveguide. The shorted turn resistance of the shield surrounding the coil is much larger than the shorted turn resistance of the waveguide because of its high resistivity and permeability. It therefore has negligible influence on switching speed.

Experimental measurements were conducted to determine the accuracy of the shorted turn circuit model just described. Figure 6 compares the theoretical and experimental results of switching time constant plotted against waveguide silver plating thickness. It is suspected that

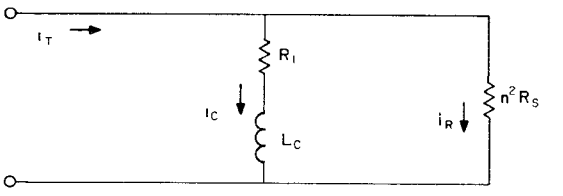

Fig. 5. Circuit model for shorted turn effects.

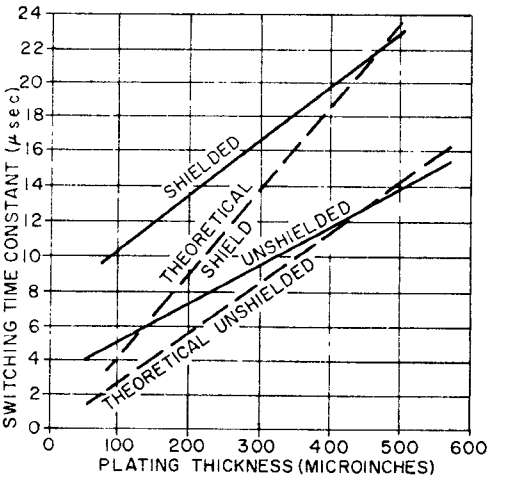

Fig. 6. Plating thickness vs. switching speed.

the difference between theoretical and experimental curves at thin plating thicknesses was due to the inability to accurately deposit or subsequently measure plating thinner than 200 microinches.

The difference in switching time constant between a shielded and unshielded phase shifter is due to the difference in L_c for the two conditions. The presence of the shield increases the measured coil inductance by a factor of 1.7 by providing a more efficient magnetic circuit.

From Fig. 6, a 3 time constant switching speed of 30 microseconds has been achieved experimentally using 100 microinches of pure silver as a waveguide. At X-band, the microwave skin depth is 26 microinches so that there is negligible RF insertion loss from the thin circular waveguide. Using silver paint with a resistivity of about 5 to 10 times higher than that of silver gives a measured 3 time constant switching speed of about 6 microseconds as shown in Fig. 7. At the same time an extra 0.2 dB of dissipation occurs in the phase shifter due to the higher wall losses in the circular waveguide.

The measured phase vs. time curve in Fig. 7 is the video detected output of an X-band phase bridge with the CP phase shifter located in one of its two arms. At $t=0$ and $t=18$ microseconds in the oscillogram, the phase bridge output is zero corresponding to the phase shifter changing from 0 to 360 degrees, respectively. The numbers 10 and 20 marked on the scope face represent 10 and 20 degrees phase deviation from the center horizontal line on the oscilloscope reticle.

The energy (U) required to switch the phase shifter from 0 to 360 degrees is 50 microjoules. This has been computed by graphically evaluating the integral:

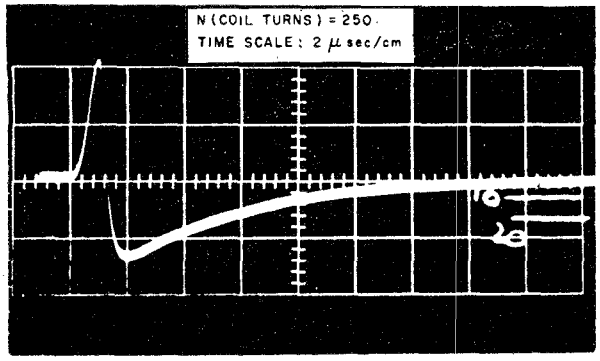

(a)

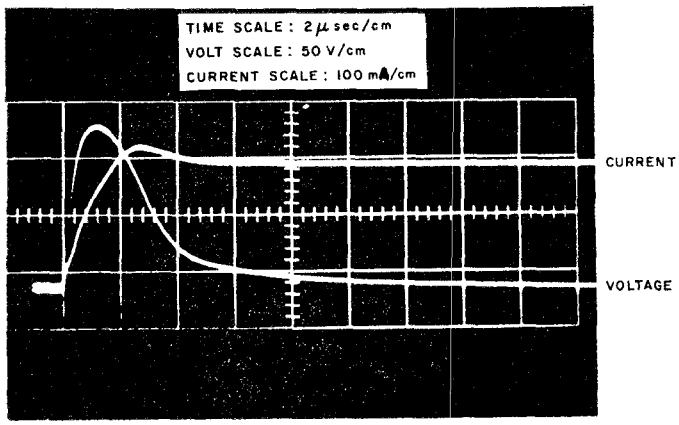

(b)

Fig. 7. Switching waveforms. (a) RF phase vs. time for 6μs switching speed and 360° phase change. (b) Coil voltage and current vs. time.

$$U = \int_0^{14} i(t)v(t)dt$$

and subtracting the dc copper losses over the same time interval. The time dependent terms v and i are taken from the oscilloscope trace in Fig. 7. The upper limit of the integral 14 is time in microseconds. Energy to switch 360 degrees can also be calculated by $\frac{1}{2}LI_m^2$ where L is the coil inductance measured on an impedance bridge and I_m is the maximum coil current needed to obtain 360 degrees of phase range. Since a linear phase vs. current characteristic is desired, the coil must be a linear inductor.

Insertion Loss

The insertion loss of the phase shifter used in the 1300-element array was 0.7 dB. About 0.25 dB of this was due to the dielectric insertion phase trimming section and conduction losses in the silver painted waveguide wall.

Using silver, fired onto the outer surface of the quartz cylinder, the insertion loss of the phase shifter would be less than 0.5 dB using Raytheon's RX1 material. If YIG (G113) were used, the insertion loss would be about 0.3 dB but the phase-current hysteresis loop would be twice as large and peak power threshold lower. This 0.3 dB loss still includes some loss in the microwave short circuit. It is estimated that a transmission-type phase shifter (no short circuit), with a linear phase-current characteristic, can be constructed using low loss YIG that exhibits an insertion loss of less than 0.2 dB.

Temperature Sensitivity

The temperature dependence of the CP phase shifter from −30°C to +85°C is described in Fig. 8. Close scrutiny of the curves in Fig. 8 will show that the insertion phase-temperature sensitivity near zero field (10 mA) is 0.7°/°C, and at maximum coil current of 177 mA (360 degrees), is 0.45°/°C. If all the curves in Fig. 8 were parallel to one another, and the temperature differences between phasers in an operating array were kept to zero, array antenna errors due to temperature effects would be zero regardless of the ambient temperature in which the antenna finds itself. An upward shift of the phase-current curve in Fig. 8 simply represents an equal-line length change in each of the phasers operating in the array and has no influence on antenna performance.

To the degree that the temperature curves are not parallel, antenna-aperture phase errors will result even with a constant temperature across this aperture. The effect of these errors is made sufficiently small by performing antenna beam collimating in the phase shifters. Temperature produced phase errors now become random and are not the major contributor to total antenna aperture rms phase error.

During the heat transfer design of the 1300-element array it was found to be a relatively simple matter to keep the temperature difference between phase shifters to less than 10°C under all environmental ambient temperatures and radar operating conditions. This means that little antenna performance degradation will occur over an environmental ambient temperature from −30°C to 85°C.

The insertion phase, as well as other performance parameters of all ferrite devices, changes with temperature due to the changing microwave permeability of the magnetic material. For larger values of applied magnetic field, the CP phase shifter exhibits a temperature sensitivity as shown in Fig. 9. The increase of insertion phase with temperature at zero field is caused by the 3 diagonal components of the tensor permeability ($\mu = \mu_{11}$) increasing with temperature [3], [4]. For large positive values of coil current (I_0 in Fig. 9), which corresponds to the scalar permeability of $\mu + k$, insertion phase becomes insensitive to temperature. This crossover point is created by the temperature sensitivity of k cancelling temperature variations in μ. For negative values of I_0 corresponding to the scalar permeability of $u - k$, insertion phase changes with temperature are magnified because of the sign change in scalar permeability.

The CP phase shifter operates over a coil current range between 10 and 177 mA where the two curves in Fig. 9 are quite parallel for most of the 360-degree phase range. If a circulator, differential phase shifter, or other device depending on differential phase shift for per-

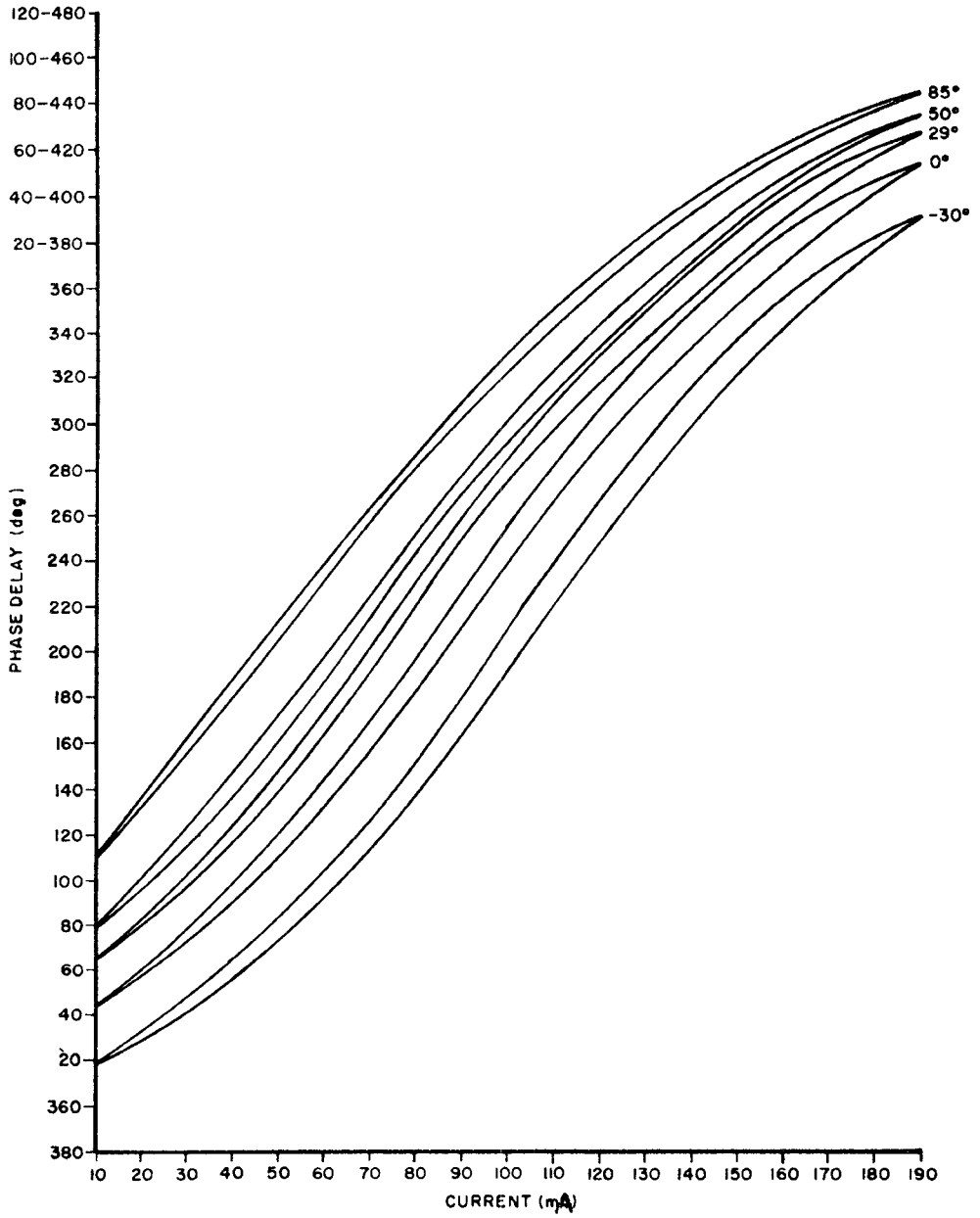

Fig. 8. Phase delay vs. current for various environmental temperatures.

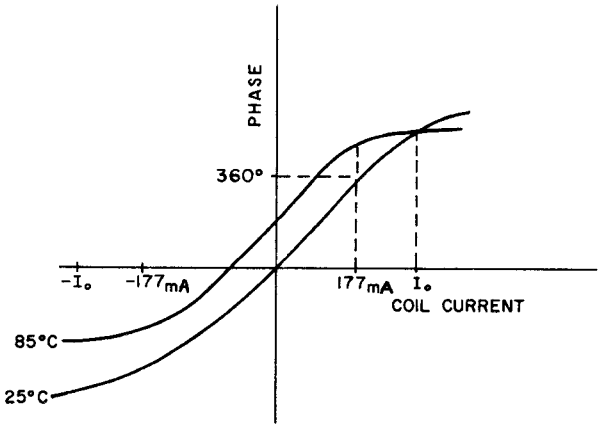

Fig. 9. Phase vs. coil current for CP phasor at two temperatures.

formance is designed to operate in this region, a temperature compensated device can result. Since this temperature insensitive operating region is below the magnetic material saturation level a little figure of merit is sometimes sacrificed.

Average and Peak Power

Average power handling capability of the CP phase shifter is determined completely by the ability to transfer heat from the phase shifter to the cooling medium used in the array. Extensive experimental measurements and heat transfer calculations have indicated that the maximum average power rating of the CP phase shifter is 35 watts. This rating is fixed by the level of RF heating in the ferrite rod. Thirty-five watts of RF power

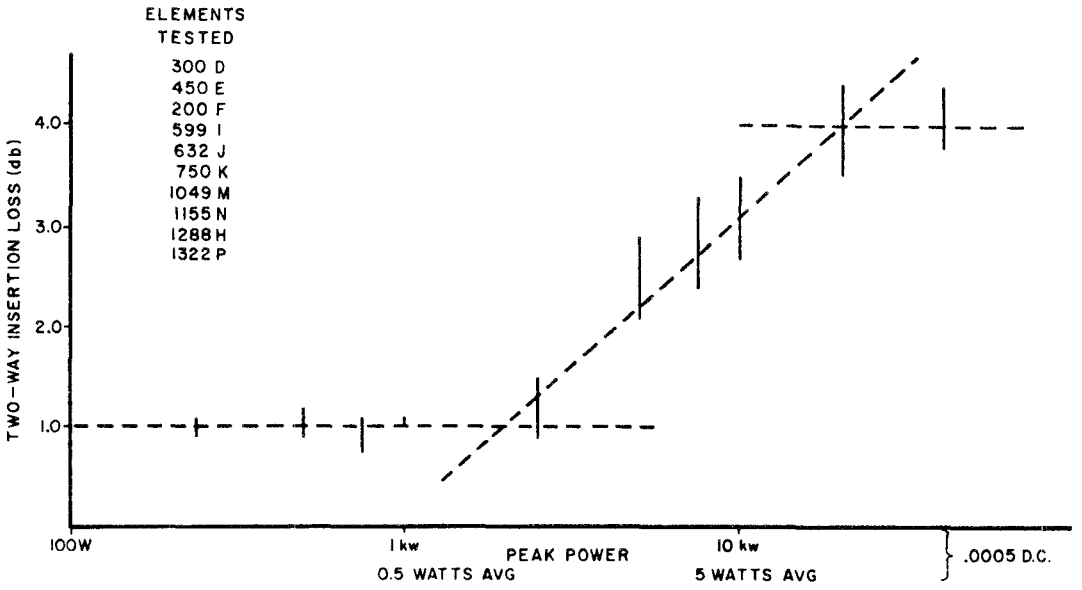

Fig. 10. Maximum insertion loss (two-way) vs. peak power.

input causes a 10-degree insertion phase change at zero field as compared to zero degrees insertion phase obtained with milliwatts of power input. The 10-degree phase change corresponds to a ferrite rod temperature of 14°C. Cooling air, moving at a moderate rate (about 700 ft³/min), passes over the outer surface of the shield under these conditions. This very closely simulates the array cooling environment. The restriction of 10 degrees phase change due to RF heating is a rather arbitrary choice even when the phaser is to be used an an array requiring an antenna aperture taper with a null at the edge. In this case the 10-degree phase change at the center elements causes only a slight antenna beam defocus. If this restriction were relaxed, and it can be in most applications, the phase shifter could be rated at much higher than 35 watts. Further, if the phaser were used in an antenna utilizing a uniform aperture distribution where equal power is dissipated in each array element, much greater than 35 watts average power can be handled.

For a 1300-element array having a 10-dB aperture edge taper, 35 watts at the center element corresponds to a radar transmitter average power of about 13 kW.

Ferrite materials exhibit a power vs. insertion loss nonlinearity [5] when operating at, or below, ferromagnetic resonance. When the peak power in a particular ferrite material is increased above a certain threshold, the insertion loss rises very rapidly. The power level at which this threshold occurs depends on the composition of the ferrite material, as well as its geometry, and the geometry of the transmission line in which it is located. For any given ferrite material there is a critical or threshold value of internal RF magnetic field intensity (h_c) which is invariant with geometry, and above which insertion loss rises sharply.

The CP phaser geometry is such, that for a given input power level, the RF magnetic fields are relatively high. Therefore, an increase in insertion loss occurs at relatively low power levels.

The peak power handling capability of ten phase shifters selected and tested from a group of 1400 is illustrated in Fig. 10. The letters following the serial number in the figure refer to the firing lot from which the ferrite rod was selected. The loss values include the loss of the test fixture and, therefore, have a slightly higher average value than that due to the phase shifter alone. The onset of high power nonlinearity occurs at approximately 2.0 kW for all phase shifters. The vertical lines plotted represent the spread of measured insertion loss for the ten elements at the various peak power levels.

Straight YIG (Trans-Tech G113) exhibits a nonlinearity threshold of about 900 watts when used in the same phase shifter design.

Bandwidth

Two frequency sensitive parameters of the CP phase shifter can be measured directly. These parameters are first, nonlinearity; second, and more significant, the slope of the phase-current characteristic. The nonlinearity of the phase-current characteristic is a function of the ferrite material and input mismatch of the phase shifter. A 360-degree reflection phase shifter with a linear phase-current curve and perfect input match is plotted in Fig. 11 as a dotted straight line. If the input reflection coefficient Γ is nonzero, the measured phase-current curves depart from linear with the maximum departure of $2|\Gamma|$ [6], [7]. The shape of this deviation from linear, or nonlinearity error, has a sinusoidal appearance. Phase deviation due to the shape of the minor B-H loop of the ferrite rod also has approximately the same sinusoidal shape. Therefore, at a single frequency, it is nearly impossible to separate the nonlinearity effects due to imperfect element match from nonlinearity effects due to the shape of the magnetization curve. As frequency is

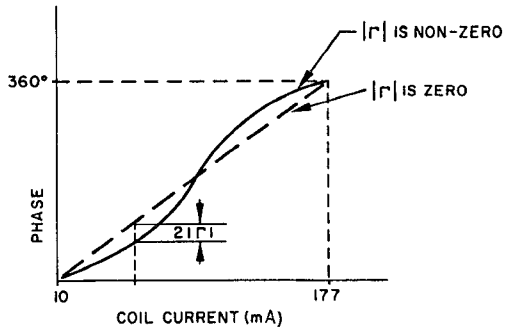

Fig. 11. Phase vs. coil current for a linear phasor with zero and nonzero input reflection coefficients.

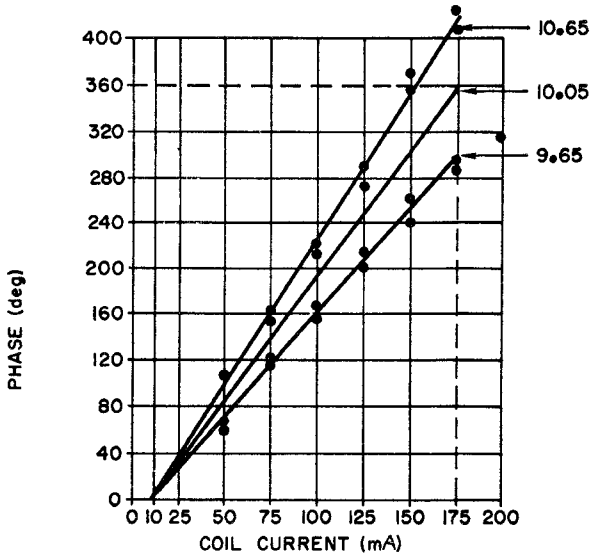

Fig. 12. Phase vs. coil current at three frequencies for element no. 36E.

changed, however, the two contributors to nonlinearity error begin adding and cancelling as the phase of the input reflection coefficient changes.

Since the total phase deviation from linear is approximately a sinusoid, it can and should be treated as an imperfect element input match rather than an item in the phased array error budget, even if it is caused in part by the shape of the magnetization curve. This argument is even more convincing when one realizes that the actual element impedance in an array environment is strongly influenced by the ever present mutual coupling between neighboring elements. As the mutual coupling changes with scan angle, so does element or phase shifter input VSWR.

The most significant phase-error contributor over frequency is the phase-current slope change. Figure 12 is the measured phase vs. current curves at three frequencies within the 10-percent band. (A best fit straight line has been drawn through the plotted experimental points. In the interest of clarity these points have been

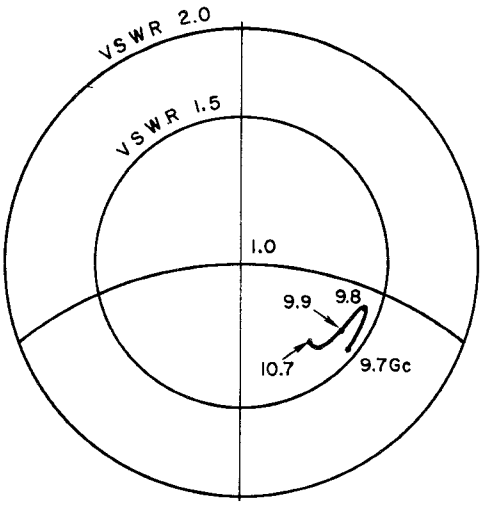

Fig. 13. Smith Chart impedence vs. frequency of the near broadside simulator.

omitted for the center design frequency of 10.05 GHz.) From the viewpoint of antenna performance, these slope errors have an undetectable influence on beam pointing error over the 10-percent frequency band. The negligible effect on beam pointing accuracy is again due to beam collimating with phase shifter control which randomizes phase-current slope errors.

Later phase shifter design improvements have shown that this slope sensitivity can be reduced by more than a factor of 2 using larger ferrite rod diameters.

IV. Radiating Element

The radiating element was empirically designed to have better than a 1.10 VSWR at center band when energy was radiated from an array element surrounded by terminated and inactive neighboring elements. Square element spacing was used with 0.700 inch between centers. This radiating element design method is deficient in that it ignores VSWR influences of mutual coupling between elements.

A more meaningful method of designing radiating elements is to use waveguide phased array simulator techniques developed by Wheeler Laboratories, Great Neck, N. Y. [8], which take into account the effects of mutual coupling. A four-element simulator, launching the TE_{10} mode, was constructed to test the radiating element design mentioned above. This waveguide simulator simulated an H-plane polarized beam scanned to 12 degrees in the cardinal symmetry plane of the array. Figure 13 is the element impedance vs. frequency as measured in the near broadside simulator. Notice that the element impedance went from less than 1.10 to about 1.40 at center frequency when the effects of mutual coupling are taken into account. The difference would be even more dramatic had the element spacings been smaller. A slight modification of radiating element geometry would move the cluster of points in Fig. 13 closer to the center of the Smith Chart.

Figure 13 refers to the behavior of only the radiating element impedance. The VSWR of the impedance transformer between the dielectric phase trimmer (see Fig. 1) and the ferrite rod was under 1.25 from 9.7 to 10.7 GHz. Improved phase shifter designs have combined the two transformers into one, forming an integrated phase shifter and radiating element.

V. Phase Shifter Accuracy and Reproducibility

A total of 1400 CP phase shifters were constructed and tested to determine their acceptance and reproducibility. The trimmed phase-current characteristic averaged over 1400 phase shifters is shown in Fig. 14. Each characteristic was measured after first cycling coil current from 10 mA to 190 mA. The average hysteresis loopwidth is 15.5 degrees and occurs at 121 mA. The linearity of the characteristic is within ± 12 degrees over a 360-degree range including hysteresis effects. The data presented in the figure was taken at 10.125 GHz. A coil current of 177 mA was chosen because the straight line it produces causes the element phase error to have equal positive and negative values of 12 degrees. Further, it causes the average error curve to be nearly sinusoidal. As mentioned earlier this sinusoidal-error term can then be treated as an array front-face mismatch, and consequently will not contribute to the rms or systematic phase inaccuracy quoted for the ferrite phase shifter element.

It is important that all phase shifters in the array be of the same overall electrical length at 10 mA of coil current. Absolute length variations at this current level are primarily the result of ferrite material nonreproducibility and variations in ferrite rod diameter.

Experimental measurements indicate that the ferrite diameter is a critical dimension. It was found that a change of 0.0015-inch in the ferrite diameter caused an absolute length change of 29 degrees. The machining tolerance specification on the ferrite diameter was ± 0.0003-inch, although the majority of pieces were closer to the nominal dimension. Dielectric constant variations in the material surrounding the ferrite can also cause phase variation. However, little problem in this respect was observed since the dielectric constant of quartz is 3.84 ± 0.01.

Figures 15 and 16 are histograms of the insertion phase distribution for an applied field of 10 mA before and after phase trimming. Figure 16 shows the improvement in the distribution after trimming. The total width of the distribution has been improved by a factor of three. At other values of applied field, the distribution will be seen to increase as a result of the presence of hysteresis and nonreproducibility of phase-current slope. Future phase shifter models will not require insertion phase trimming due to improved methods of ferrite material preparation and the availability of a better CP phase shifter design which has a shorter electrical length.

Figure 17 is a plot of the static or measured standard deviations for phase distributions at different values of current. The curve σ_1 is the standard deviation for the upper curve of Fig. 14 and σ_2 is the deviation for the lower curve. The top curve of the loop has a larger standard deviation than the bottom loop. Apparently, the phase current characteristic is better defined for increasing current than decreasing current.

From a statistical point of view it can be reasoned that phased array aperture error contributions, due to CP phase shifter hysteresis effects, is negligible in light of the more dominating but certainly acceptable reproducibility errors. In the case of the operation of a large group of these phase shifters in an array, the direction and magnitude of magnetization from which a particular phase command is approached is random. Therefore, it is highly unlikely, and an extreme case, that a phase shifter in the array will operate on its measured, static, phase-current curve, which can be called in this context a major hysteresis loop. It is much more likely that a phaser operates on some minor hysteresis loop which is within the bounds of the major loop.

The rms antenna-difference pattern beam pointing error for the 1300-element array was measured to be somewhat less than 1.2 milliradians or 2.4 percent of the broadside beamwidth. The rms pointing error was the same at every frequency within the 10 percent frequency band of interest. Far out rms sidelobes were also greater than 40 dB down at all frequencies. This antenna performance appears to agree rather well with what published theory predicts the antenna performance should be in terms of phase shifter accuracy.

VI. Conclusion

A phaser has been described which imparts nonreciprocal phase shift to incoming circularly-polarized waves. A planar array antenna was constructed and tested using 1300 of these phase shifters, the results of which demonstrated the suitability of such a device for use in phased array antenna applications. The following comments briefly summarize the more outstanding salient features of a CP phase shifter when used in a phased array antenna.

1) Good phase setting accuracy is obtainable. In an operating array, aperture phase errors due to phase shifter nonreproducibility or inaccuracy is less than 7 degrees rms. Insertion phase temperature sensitivity is also low, 0.70 to 0.45 degree per degree C, between phase setting of 0 to 360 degrees, respectively.

2) This type of phaser makes possible a phased array configuration utilizing a nonreciprocal phase shifter but with no need of magnetic field reversals between transmit and receive modes of radar operation.

3) If desired, the array antenna can be made to reject rain clutter [9] by reversing the magnetic fields in each array element between transmit and receive. Reversing magnetic fields "tunes" the antenna beam to the double

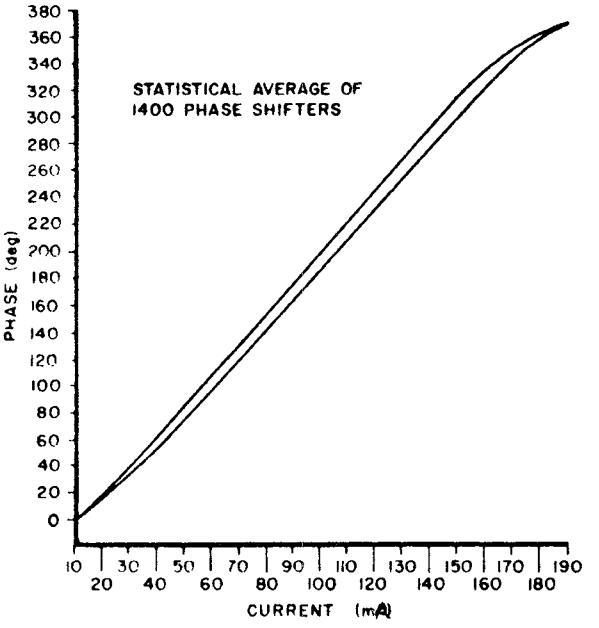

Fig. 14. Measured phase vs. current.

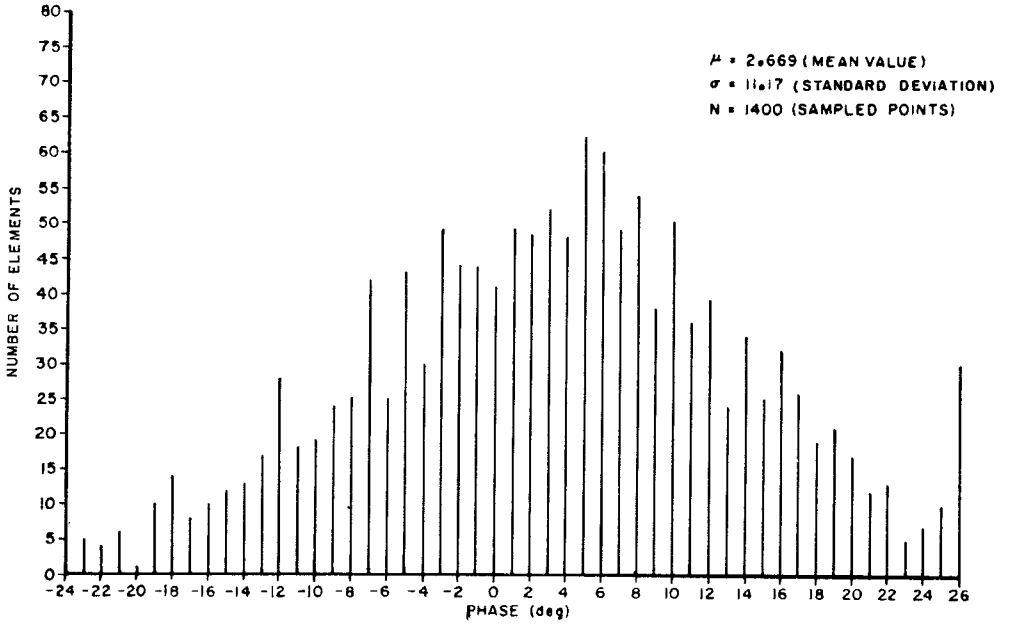

Fig. 15. Phase distribution for 10 mA applied field—before trimming.

bounce radar return. Because of the nonreciprocal properties of the phaser no antenna beam is formed for the single bounce return. A circularly-polarized planar phased array antenna, with high quality circular polarization at beam broadside, becomes elliptically polarized when scanned far from broadside. The amount of ellipticity in the transmit and receive beams degrades rain clutter rejection ability. This degradation is less if nonreciprocal array elements make up the array than if reciprocal elements are used.

4) The switching energy to obtain 360 degrees of phase shift is the same or lower than that reported for many ferrite digital-latching phase-shifter designs.

5) This type phaser can be used to construct a transmission or reflection array. A reflection array configuration permits simple solutions to problems dealing with element driver packaging, electrical interconnections, and element air cooling. This, coupled with a simple phase shifter form factor, gives rise to a low-cost, highly-reliable beam steering element.

This CP phase shifter design concept has been successfully demonstrated at frequencies from 3 to 18 GHz. Using newly discovered design techniques a method has been found to make the CP phase shifter both reciprocal and polarization insensitive. This PIP shifter (Polarization Insensitive Phase Shifter) has been designed with figures of merit better than 360 degrees phase range for 1 dB insertion loss.

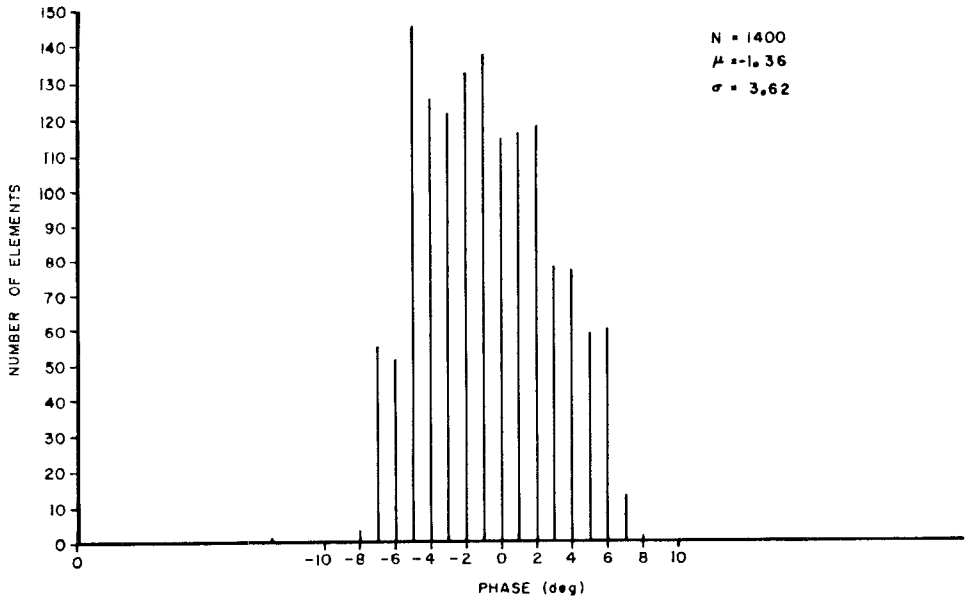

Fig. 16. Phase distribution at 10 mA applied field—after trimming.

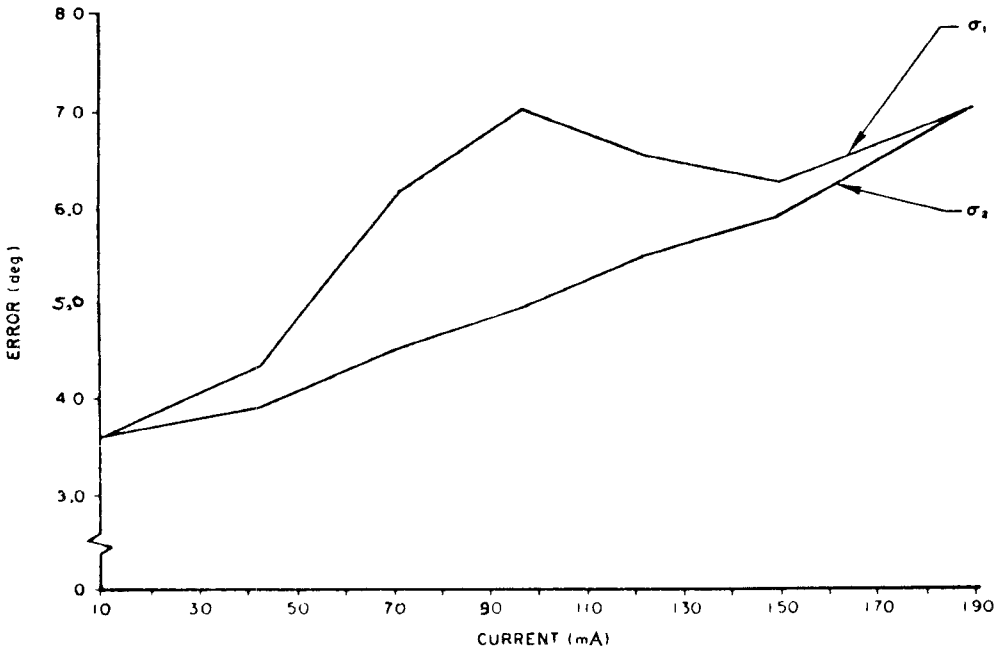

Fig. 17. Standard deviations for phase distributions at different values of current for 1400 phase shifters.

Acknowledgment

The authors are indebted to F. O'Hara, W. McLeod, and others, who made significant contributions during the early days when this phased array technique was first conceived. A tribute is also due J. Chapman, who was responsible for the phase shifter and array mechanical design.

References

[1] H. Scharfman, "Three new ferrite phase shifters," *Proc. IRE*, vol. 44, pp. 1456–1459, October 1956.
[2] A. G. Fox, S. E. Miller, and M. T. Weiss, "Behavior and application of ferrites in the microwave region," *Bell Sys. Tech. J.*, January 1955.
[3] J. Nemarich and J. Cacheris, "Temperature dependence of microwave permeabilities for polycrystalline ferrite and garnet materials," Diamond Ordnance Fuze Labs., Washington, D. C., DOFL Rept. TR-647, October 3, 1958.
[4] R. C. LeCraw and E. G. Spencer, "Tensor permeabilities of ferrites below magnetic saturation," *IRE Conv. Rec.*, pt. 5, vol. 4, pp. 66–74, 1958.
[5] H. Suhl, "The nonlinear behavior of ferrites at high microwave signal levels," *Proc. IRE*, vol. 44, pp. 1270–1284, October 1956.
[6] J. Reed, "Long line effect in pulse compression radar," *Microwave J.*, vol. 4, p. 99, September 1961.
[7] G. E. Schafer, "Mismatch errors in microwave phase shift measurements," *IEEE Trans. on Microwave Theory and Techniques*, vol. MTT-8, pp. 617–622, November 1960.
[8] P. W. Hannan and M. A. Balfour, "Simulation of a phased-array antenna in waveguide," *IEEE Trans. on Antennas and Propagation*, vol. AP-13, pp. 342–353, May 1965.
[9] M. I. Skolnik, *Introduction to Radar Systems*, New York: McGraw-Hill, p. 456.